Unusual Structures in Single-Stranded Ribonucleic Acid: Proton Nuclear Magnetic Resonance of AUCCA in Deuterium Oxide†

Michael P. Stone, Diane L. Johnson, and Philip N. Borer*

ABSTRACT: Conformational features of the oligoribonucleic acid (oligo-RNA) A^1-U^2-C^3-C^4-A^5 are explored by proton nuclear magnetic resonance (NMR). The sequence is a molecular cognate of a portion of the TψC loop and stem regions of yeast $tRNA^{Phe}$. The molecule forms at least two classes of flexible yet ordered structures. Class I states are similar in spectral properties to the component oligomers, AU, AUC, and AUCC, and are likely to be standard right-helical structures. Class II states are characterized by a 2′-endo pucker at A^1 and unusually large shielding of several C^3 and U^2 protons. Most of these features are consistent with identifying the class II solution structures with the "arch" conformation for the TψC region determined by X-ray crystallography of yeast $tRNA^{Phe}$.

Single-stranded oligoribonucleotides form loosely ordered structures at low temperatures in aqueous solution; usually it has been found that the nucleotide chain is a right-hand helix with the aromatic bases stacked upon each other. The conformation of the ribose rings in the nucleic acid backbone can be approximated by a two-state equilibrium between the ^3E and ^2E (3′-endo and 2′-endo) sugar conformers (Rich et al., 1979; Sundaralingam, 1974; Ts'o, 1974). The predominant form for the ribose rings in ribonucleic acid (RNA)[1] is the ^3E conformation in oligomers with a high degree of stacking (Borer et al., 1975).

There is spectroscopic evidence that alternative ordered structures exist for single-stranded RNA in solution. Gray et al. (1972) studied the circular dichroism (CD) spectra of several trinucleotides containing internal uridine residues. These molecules had CD spectra which could not be explained on the basis of nearest-neighbor stacking interactions. Lee & Tinoco (1980) have continued this study on trinucleotides by using ^1H NMR methods, as have M. P. Stone, P. N. Borer, G. D. McFarland, S. A. Winkle (unpublished experiments) by using ^{13}C NMR; it is apparent that ordinary right-helical structures do not conform to the data. Uhlenbeck et al. (1973) measured CD spectra of $A_6C_mU_6$ oligomers[1] with $m = 4$–8; these oligomers form hairpin loop structures with a single-stranded -C_m- region. For $m \geq 6$ the CD spectra of the -C_m- portion closely resemble oligo-C_m spectra, but a different structure occurs for $m \leq 5$.

Studies of the crystal structure of yeast $tRNA^{Phe}$ by X-ray diffraction showed that certain single-stranded oligonucleotide sequences in the loop portions form unusual, non-right-hand stacked conformations (Rich et al., 1979; Stout et al., 1978; Quigley & Rich, 1976). ^1H NMR studies have shown that the $tRNA^{Phe}$ molecule apparently conforms to the same three-dimensional structure in solution (Kan et al., 1977; Kearns, 1977; Reid & Hurd, 1977). It is likely that these unusual loop structures are common features of tRNA since the critical sequence elements are conserved among the various tRNAs thus far sequenced. It would seem that these nucleotide sequences must be crucial to the structure and the function of the molecule.

Within the TψC loop, residues m^1A58, U59, C60, C61, and A62 form what Quigley & Rich (1976) call an "arch" in which U59 and C60 are excluded from the stacking domain formed by m^1A58, C61, and A62. In this structure, the ribose ring of m^1A58 is found to be in the ^2E conformation rather than the ^3E conformation normally expected for right-hand stacked oligoribonucleotides. Three groups subsequently published refined structures of $tRNA^{Phe}$ based on X-ray data at 2.5–3.0-Å resolution (Stout et al., 1978; Hingerty et al., 1978; Holbrook et al., 1978). In each case the ^2E conformer is found at residues 58 and 60, with ^3E at residues 59, 61, and 62. The unusual stacking arrangement is similar in each study and is further stabilized by non-Watson–Crick hydrogen bonds in the backbone (Figure 1a). The arch and other interesting oligomer sequences, labeled "U-turns" because of the importance of the uridine residue in forming the structure, occur in various single-strand regions of the crystal structure.

The question arises: Can these specific sequences spontaneously form unusual conformations in solution, or are the features characteristic only of the intact tRNA molecule? These unusual structures could play an important role in enzyme recognition of important sites on mRNA or tRNA. Furthermore, single-stranded structures should be more easily deformed than double helices and may confer an important degree of flexibility in an induced-fit interaction between protein and nucleic acid.

We undertook this study to determine whether the oligonucleotide AUCCA could mimic any of the structural features of the arch conformation proposed for tRNA. The oligomers AUC, AUCC, and AUCCA were synthesized enzymatically by using polynucleotide phosphorylase. All 15 nonexchangeable protons of AUCCA were assigned, and a study of the temperature dependence of chemical shift and ribose H1′–H2′ coupling indicates that this molecule exists in at least two loosely ordered conformational states in solution at low temperatures. The class I states resemble ordinary right-helical structures and probably dominate the population of ordered molecules. The class II states are characterized by a ^2E ribose pucker at A^1 and unusually large shielding of C^3H5, C^3H6,

† From the Department of Chemistry, University of California at Irvine, Irvine, California 92717. *Received October 23, 1980.* This work was supported in part by a grant from the National Institutes of Health (GM-24494). Grants from the National Science Foundation (CHE 79-10821 and MPS 75-06152) provided funds for the Bruker WM-250 and WH-90 spectrometers.

[1] Abbreviations used: none of the oligonucleotides discussed in this paper have terminal phosphates; we abbreviate the notation for oligomers by leaving out the phosphodiester linkage; RNA, ribonucleic acid; tRNA, transfer RNA; mRNA, messenger RNA; Hepes, 4-(2-hydroxyethyl)-1-piperazineethanesulfonic acid; DEAE, diethylaminoethyl; EDTA, ethylenediaminetetraacetic acid; DSS, sodium 4,4-dimethyl-4-silapentanesulfonate; FT, Fourier transform.

0006-2960/81/0420-3604$01.25/0

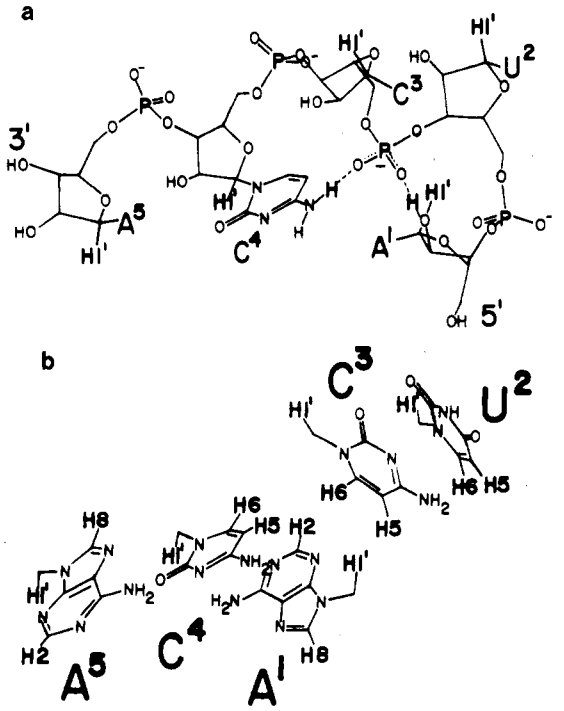

FIGURE 1: Arch conformation for AUCCA proposed by Quigley & Rich (1976) (adapted from their stereo drawing labeled Figure 6): (a) the ribose–phosphate backbone; (b) the base stacking arrangement. The H1′ and C^4 appear in both (a) and (b) and serve as points of reference for comparison. In yeast $tRNA^{Phe}$ AUCCA would correspond to residues 58–62, C^4 and A^5 would be Watson–Crick hydrogen bonded in the TψC stem, and A^1 would be involved in a tertiary hydrogen bond to rT in the TψC loop. In almost all tRNA species the nucleotides corresponding to A^1 and C^4 are invariant, and C^3 corresponds to a constant pyrimidine locus.

C^3H1′, and U^2H1′. Most of these features are consistent with identification of the class II states as arch conformations.

Materials and Methods

(*A*) *Synthesis of Oligonucleotides.* The dimer ApU was obtained as the ammonium salt (Sigma Chemical Co.) and used without further purification. Chain extension was achieved enzymatically by using primer-dependent polynucleotide phosphorylase (PNPase P) obtained by trypsin digestion of the primer-independent enzyme (P-L Biochemicals; Klee et al., 1967).

For AUCC, a solution (25 mL) containing 3.0 mM ApU, 6 mM CDP, 10 mM $MgCl_2$, 0.8 M NaCl, 0.2 M Hepes, pH 8.2, and 20% v/v PNPase P was incubated for 5 days at 37 °C. For AUCCA, a solution (8.3 mL) containing 1.0 mM AUCC, 20 mM ADP, 10 mM $MgCl_2$, 0.8 M NaCl, 0.2 M glycine, pH 9.2, and 5% v/v PNPase P was incubated for 5.5 h at 37 °C.

Each mixture was then heated to 80 °C for 5 min to inactivate PNPase P and treated with alkaline phosphatase (calf intestine, Boehringer) to hydrolyze the nucleoside diphosphate. The oligonucleotides of interest were then separated from their respective mixtures on DEAE-Sephadex A-25 columns, Cl^- form, using a 3.0-L 0–0.8 M NaCl gradient in 0.01 M Tris, pH 8.2. Fractions eluting from the column were monitored by absorbance at 260 nm, and their identity was verified by high-pressure liquid chromatography (Waters μBondapak C_{18} reverse-phase column, 2–12% acetonitrile gradient in 1% ammonium acetate–H_2O, 10 min; McFarland & Borer, 1979) and paper chromatography (descending mode, 70:30 ethanol–1 M ammonium acetate). Appropriate fractions were desalted by passage through a Bio-Gel P-2 column, with millipore-filtered H_2O. Samples were evaporated and quantitated by absorbance at 260 nm. Extinction coefficients at 25 °C were 38.3 for AUCC and 52.1 A_{260} units/μmol of strand for AUCCA (Borer, 1975).

(*B*) *NMR.* Each NMR sample contained 1.0 μmol of oligomer in 0.5 mL of 0.01 M phosphate buffer, pH 6.6, and 10^{-4} M EDTA. Exchangeable protons were replaced by dissolving samples in 99.7% D_2O and evaporation, a procedure which was repeated 3 times. This D_2O was first distilled in glass because it leaves a substantial residue after evaporation. (We have tried several suppliers and all have a similar residue.) Finally the samples were dissolved in 99.98% D_2O (Aldrich), and 5 μL of 4.5 M *tert*-butyl alcohol in D_2O solution was added as an internal reference; shifts were reported with respect to DSS as described in Borer et al. (1975).

Spectra were obtained on various spectrometers, operating in the quadrature FT mode. For the Bruker WH90 spectra at 90 MHz, 600–1000 pulses were accumulated at a repetition rate of 5 s and sweep width of 900 Hz. For Varian HR-220 spectra at 220 MHz, 100–500 pulses were accumulated at a repetition rate of 3 s and sweep width of 2500 Hz. For Bruker WM-250 spectra at 250 MHz, 8–100 pulses were accumulated at a repetition rate of 4 s and sweep width of 2500 Hz. For Nicolet 360-MHz spectra, 1–100 pulses were accumulated at a repetition rate of 4 s and sweep width of 4000 Hz. A 30–50° flip angle was used in all cases. Except at the highest temperatures, relaxation times were sufficiently rapid so as to not require any additional delay after data acquisition. Temperatures were verified by reference to methanol or ethylene glycol standards (Van Geet, 1968, 1970).

Results

Assignment of Resonances. A 360-MHz ^{1}H NMR spectrum of AUCCA is shown in Figure 2 at 30 °C. Only signals from the base and ribose 1′ protons are displayed. The remaining ribose proton signals are overlapping multiplets, some of which are obscured by the residual HDO peak. Assignments were made by comparing spectra at 70 °C following the incremental assignment scheme described by Borer et al. (1975).

Assignment of the 15 proton resonances of AUCCA represents a tremendous challenge to our understanding of the spectral features of oligonucleotides. A total of 11 of the 15 signals are doublets, meaning that each spectrum is the superposition of 26 lines in the 5.5–8.5-ppm range. Our assignments result from a careful comparison of over 50 NMR spectra as a function of temperature and oligomer chain length; at least they represent an internally consistent analysis, and are probably as good as any which can be obtained by indirect methods.

Assignments were made on the basis of some well-known general features of NMR spectra of oligo-RNA. These features include the ~8-ppm location of the H6 doublets and the H2 and H8 singlets, the ~6-ppm chemical shift of the H5 and H1′ doublets, temperature-invariant coupling constants of 7.6 Hz for H5 and H6 of cytosine and 8.1 Hz for uracil, variable coupling constants in the range of <1–6 Hz for ribose H1′ signals which decrease with decreasing temperature, and much shorter T_1 relaxation times for H8 in comparison to H2. Finally, ring-current shielding is known to decrease in the order A > G > C > U. For details of the assignment procedure see Appendix.

Temperature Dependence of AUCCA Spectra. The temperature-dependent shielding effects are shown by the *open symbols* in Figures 3 (the base protons) and 4 (the H1′) over the full 3–80 °C range. The largest decreases in shielding throughout the order–disorder transition are roughly 0.3 ppm for the U^2-, C^3-, and C^4H5 and -H1′ signals. Also, A^1- and

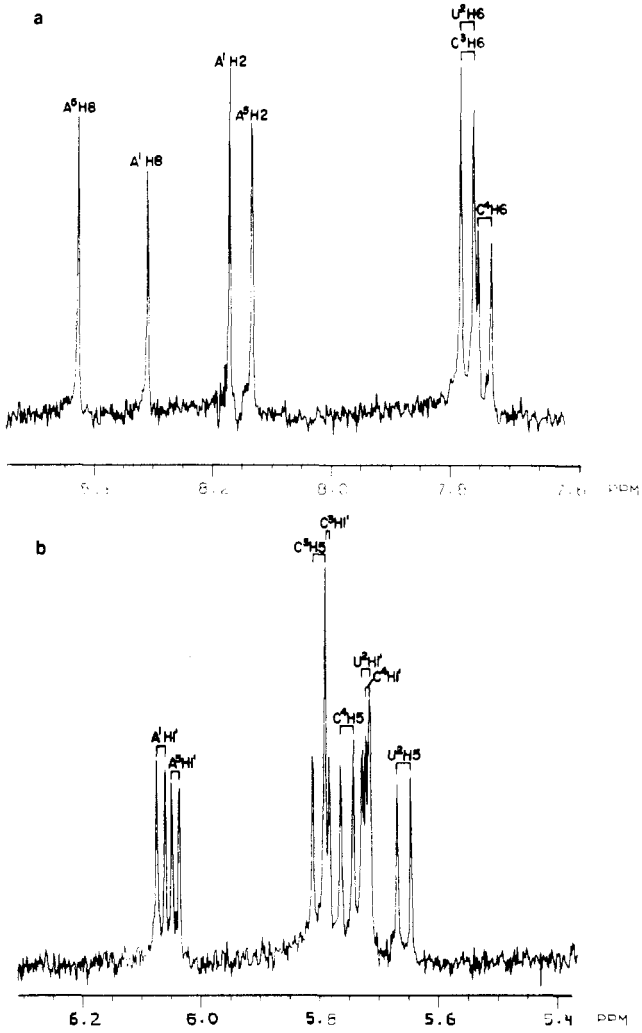

FIGURE 2: A 360-MHz ^{1}H NMR spectrum of 2.0 mM AUCCA in 10 mM phosphate, pH 6.6, 0.1 mM EDTA, and 99.98% D_2O at 30 °C. (a) The H8 H2, H6 region; (b) the eight H1′ and H5 doublets. The FT spectrum from 16 transients, 8K real data points. Chemical shifts are in ppm from DSS.

Table I: $J_{1'-2'}$ (Hz) vs. Temperature for AUCCA and AUCC

	AUCCA				AUCC			
	3 °C	10 °C	40 °C	76 °C	3 °C	10 °C	40 °C	76 °C
A^1	*4.5*	4.6	5.2	5.3	*3.4*	3.6	4.6	5.2
U^2	2.4	3.2	4.0	4.2	3.0	3.3	4.4	5.2
C^3	<1	1.1	3.0	4.2	1.8	2.1	3.4	4.4
C^4	<1	1.8	4.0	4.1	2.4	2.6	3.5	4.1
A^5	*2.6*	3.7	4.5	5.8				

A^5H2 show a moderately large decrease. There are several resonances which shift very little or even become slightly more shielded on increasing the temperature: A^1- and A^5H8; U^2-, C^3-, and C^4H6; A^1- and A^5H1′. The H1′–H2′ coupling constants all increase with temperature (see Table I); there are uncharacteristically large values of $J_{1'-2'}$ for A^1H1′ at the lowest temperatures, however.

Chain-Length Dependence in AUCCA Series. The chain-length dependence of chemical shift for AUCCA and its 5′ fragments, AUCC, AUC, and AU, is explored in Table II at 4 and 70 °C. (Further spectral properties of the trimer and shorter oligomers are detailed in the microfilm edition of this journal; see paragraph at end of paper regarding supplementary material.) The table lists values of $\Delta\delta$, the change in resonance position of a particular proton in going from the

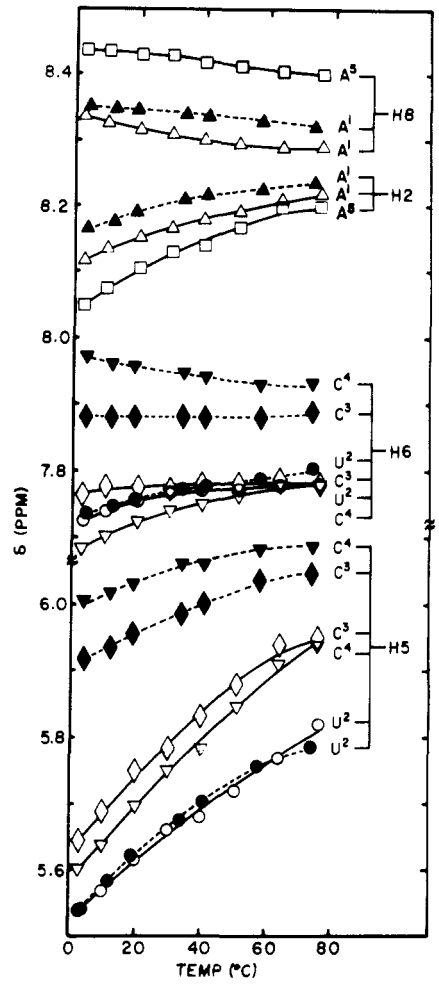

FIGURE 3: Chemical shift vs. temperature profiles for the nonexchangeable base protons of AUCCA (open symbols, solid lines) and AUCC (closed symbols, dashed lines). A^1 (△); U^2 (○); C^3 (◇); C^4 (▽); A^5 (□). Chemical shifts are in ppm from DSS.

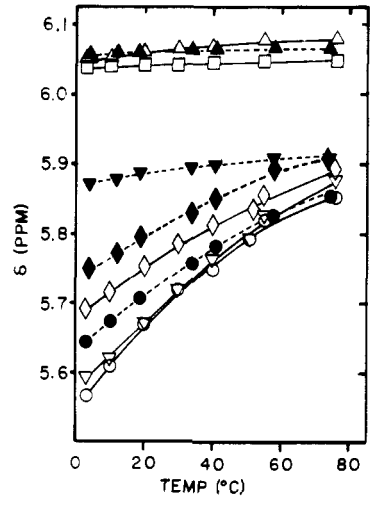

FIGURE 4: Chemical shift vs. temperature profiles for the H1′ resonances of AUCCA (open symbols, solid lines) and AUCC (closed symbols, dashed lines). A^1 (△); U^2 (○); C^3 (◇); C^4 (▽); A^5 (□). Chemical shifts are in ppm from DSS.

mononucleotide to longer chains under the same conditions of temperature, strand concentration, and ionic strength:

$$\Delta\delta = \delta_{\text{monomer}} - \delta_{\text{oligomer}}$$

Positive values of $\Delta\delta$ indicate an increase in shielding in going from monomer to oligonucleotide. For stacked structures in

Table II: $\Delta\delta$ Values (ppm) for AUCCA and Its 5′ Fragments[a]

		4 °C				70 °C			
		AUCCA	AUCC	AUC	AU	AUCCA	AUCC	AUC	AU
A^1H	8	0.18	0.18	0.18	0.18	0.16	0.13	0.15	0.14
	2	0.13	0.10	0.09	0.07	0.05	0.01	0.02	0.01
	1′	0.09	0.10	0.08	0.10	0.06	0.06	0.07	0.05
U^2H	6	0.40	0.39	0.39	0.40	0.18	0.18	0.16	0.18
	5	0.43	0.45	0.43	0.48	0.13	0.18	0.18	0.19
	1′	*0.43*	*0.36*	0.34	0.33	0.12	0.09	0.11	0.14
C^3H	6	*0.12*	*0.03*	0.04		*0.02*	*−0.08*	*−0.02*	
	5	*0.41*	*0.16*	0.23		*0.13*	*0.01*	*0.06*	
	1′	*0.25*	*0.07*	0.06		0.03	0.01	0.01	
C^4H	6	*0.22*	*−0.07*			*0.02*	*−0.13*		
	5	*0.45*	*0.07*			*0.13*	*−0.02*		
	1′	*0.41*	*0.21*			0.03	0.01		
A^5H	8	0.08				0.05			
	2	0.20				0.04			
	1′	0.10				0.08			

[a] $\Delta\delta = \delta_{monomer} - \delta_{oligomer}$. Entries in italic type indicate $\Delta\delta$ values which change more than 0.05 ppm with chain length. Measured $\delta_{monomer}$ values in ppm at 4 and 70 °C, respectively, are as follows: AH8, 8.52 and 8.45; AH2, 8.25 and 8.25; AH1′, 6.14 and 6.13; UH6, 8.12 and 7.97; UH5, 5.97 and 5.95; UH1′, 6.00 and 5.96; CH6, 7.90 and 7.80; CH5, 6.05 and 6.07; CH1′, 5.94 and 5.92.

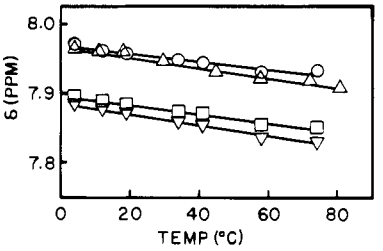

FIGURE 5: Variation of chemical shift of C^4H6 in AUCC with temperature and ionic environment. AUCC was 2.0 mM in strands in 10 mM sodium phosphate, pH 6.6, 0.1 mM EDTA, and 99.7% D_2O: no added salt (○); 0.15 M NaCl added (△); 0.15 M NaCl and 10 mM $MgCl_2$ added (□); 1.0 M NaCl added (▽). Chemical shifts are in ppm from DSS.

Table III: Shielding Increases of AUCC Protons Due to Addition of 1.00 M NaCl ($\delta_{no\ salt} - \delta_{1M\ salt}$ in ppm)

		4 °C	70 °C
A^1H	8	0.01	0.02
	2	0.01	0.02
	1′	0.00	0.00
U^2H	6	*0.05*	*0.05*
	5	0.02	0.04
	1′	0.00	0.00
C^3H	6	*0.09*	*0.09*
	5	*0.04*	*0.06*
	1′	0.00	0.00
C^4H	6	*0.09*	*0.10*
	5	*0.05*	*0.06*
	1′	0.00	0.00

solution, one normally sees an increase in $\Delta\delta$ values as chain length increases. At high temperature, these values are smaller due to decreased stacking.

For the AUCCA series the U^2 base protons have large $\Delta\delta$ values because of the large ring current of A^1, an effect which remains but is much smaller at 70 °C. Likewise, C^4 protons show dramatic shielding increases upon addition of the A^5. This effect is also much less at 70 °C. Similarly large increases for the C^3 protons occur with the addition of A^5. This large effect on the C^3 is unusual in that ring-current effects diminish with the cube of the distance away from the aromatic ring system; thus a ring-current effect from a next-nearest neighbor would not be expected to have such a large effect on C^3. Addition of A^5 to the chain also makes a small but significant change (0.07 ppm) in $\Delta\delta$ for U^2H1'.

δ vs. T profiles are plotted in Figures 3 and 4 for both AUCCA (open symbols) and AUCC (closed symbols). Most of the profiles nearly coincide at high temperatures for corresponding protons in the two oligomers. This is especially true for the H2, H8, and H1′ of A^1, U^2, and C^3 and also U^2H5 and -H6. The C^3- and C^4H5 and -H6 profiles are notable exceptions, however, differing by 0.10–0.15 ppm at high temperature where only minimal order should remain.

Effect of Salt Concentration on AUCC. Figure 5 shows the effect of salt concentration on the δ vs. T profiles of C^4H6. The profiles are nearly parallel over the whole temperature range with the 0.00 and 0.10 M NaCl curves being ~0.10 ppm less shielded than the 1.00 M NaCl and 0.10 M NaCl plus 0.01 M $MgCl_2$ curves. Table III indicates the shielding differences between the 0.00 and 1.00 M NaCl data for the other protons in AUCC. It is seen that the cytosine H6 and H5 protons are influenced most by salt, with a smaller effect on uracil H6 and negligible effects for the other protons. The same parallelism of δ vs. T profiles at various salt concentrations occurs for these other protons. No substantial effect of salt on $J_{1'-2'}$ values was found.

Discussion

Solution Conformation of AUCCA. Examination of Tables I and II suggests that a substantial population of AUCCA molecules is not stacked in a traditional right-helical structure. The evidence that nontraditional structures exist derives from coupling constant data of A^1H1' and $\Delta\delta$ values for U^2H1', C^3H1', and C^3H5.

The H1′–H2′ coupling constants reflect the population of sugar rings in the ^2E or ^3E form. $J_{1'-2'}$ is nearly 0 for the ^3E pucker and ~10 Hz for ^2E (Dhingra & Sarma, 1979), so $J_{1'-2'}$ is roughly proportional to the fraction of ^2E conformers; a coupling constant of 5 Hz means ~50% ^2E, 2 Hz means ~20% ^2E, etc. While these percent ^2E numbers must be regarded with some suspicion in an absolute sense, their relative values can be interpreted with greater confidence.

In Table I all of the J values increase with temperature, suggesting that the ^3E form of traditional stacked RNA dominates the ordered structures, giving way to an equilibrium mixture of ^3E and ^2E forms at higher temperatures. The notable exception is A^1 where the percent ^2E is a high 45% at a 3 °C and increases by only 8% at 76 °C. In contrast, A^5 undergoes a 32% increase over the same temperature interval. Therefore it appears that an important class of AUCCA

conformations at low temperature has the ribose of A^1 in the ^2E form. The terminal A^5 residue is necessary to assist A^1 in adopting this unusual conformation as the percent ^2E increases from 34% in AUCC to 45% in the pentamer at 3 °C. The ^2E ribose populations for U^2, C^3, and C^4 decrease by ~10% upon addition of A^5, the simplest interpretation being that AUCCA molecules are more rigidly constrained than those of AUCC.

A comparison of $\Delta\delta$ values for specific protons (horizontal lines in Table II) shows that most of the shielding effects are nearly constant as chain length decreases. The entries in Table II in italic type indicate those protons for which $\Delta\delta$ changes more than 0.05 ppm with chain length. Addition of A^5 to the chain should certainly shield the C^4 protons more; indeed 0.20–0.38-ppm increases in $\Delta\delta$ are observed in the 4 °C data. However, addition of A^5 shields C^3H1' an additional 0.18 ppm (almost the same as the 0.20-ppm effect on C^4H1'), C^3H5 by 0.25 ppm, C^3H6 by 0.09 ppm, and U^2H1' by 0.07 ppm (all at 4 °C). These long-range effects can be rationalized by supposing that addition of A^5 stabilizes some unusual conformation of AUCCA that is not represented in substantial population in AUCC.

The origin of the "salt effect" is not clear. Prestegard & Chan (1969) noted that high salt concentrations cause increased shielding of H6 protons of uridylic acid, with a somewhat smaller effect on H5 and very little effect on H1′. We make a similar observation of U in AUCC (Table III) but see a much larger effect with C. It is possible that the salt effect may be due to changes in the glycosidic torsion angle, changes in sugar pucker, ion binding, or perhaps even reduced water activity. The studies on AUCC suggest it is not due to changes in sugar pucker; the $J_{1'-2'}$ values and the H1′ chemical shifts vary little with salt concentration. Changes in the glycosyl angle could affect H6 via the lone-pair electrons on the ribose ring oxygen, O1′, or the phosphate anisotropy. Only the phosphate would be likely to cause differential shielding at H5 because H5 is so far from O1′. Na^+ and Mg^{2+} ions are known to associate with the phosphates, so it is likely that this is the origin of the shielding effect. We have begun experiments with cytosine nucleosides and nucleotides to try to determine the structural origin of the shielding effect.

There are sizable shielding increments at 70 °C in the C^3- and C^4H5 and -H6 upon addition of A^5 to AUCC (see italic entires in the right half of Table II). These increments are in the range of 0.10–0.15 ppm; an effect of similar direction and magnitude is seen in AUCC spectra in the presence of high Na^+ or Mg^{2+} concentration. Two AUCCA samples were prepared and desalted differently (by repeated desalting on P-2 columns or by lyophilization from ammonium acetate), and both showed identical δ vs. T profiles. We conclude that the effect on the 70 °C spectra of adding A^5 to AUCC is not due to the presence of high salt concentrations, although it is similar to the effect of adding Na^+ or Mg^{2+}. It is likely that a temperature-independent shielding increment of 0.1–0.15 ppm for cytosine H5 and H6 arises from motions of these protons with respect to the phosphate that are different in AUCCA than in AUCC.

We can now summarize our observations on the solution conformation of AUCCA. We assert that there are at least two major classes of ordered states at low temperature. The first, and probably dominant, forms are the traditional right-helical stacked structures that follow the stacking pattern observed in AU, AUC, and AUCC. The second class is characterized by the atypical ^2E ribose pucker at A^1, unusually large shielding of C^3H5 and C^3H1', and somewhat greater shielding at U^2H1' and C^3H6 than the right-helical form. The data presented here on chain-length dependence of NMR are uninformative regarding possible unusual shielding at C^4 and A^5. We plan to synthesize CA, CCA, and UCCA which in comparison with AUCCA should tell more about shielding at C^4 and A^5.

Arch Model. The arch conformation suggested by Quigley & Rich (1976) for the $m^1A^{58}U^{59}C^{60}C^{61}A^{62}$ region of yeast $tRNA^{Phe}$ is consistent with certain features of the class II AUCCA conformation noted above. The arch (see Figure 1) is built with an unusual stacking arrangement at U^2 and C^3, while A^1, C^4, and A^5 form an uninterrupted stacking domain. C^3H5 and -H6 are in close proximity to the phosphate linking U^2 and C^3 (this is the phosphorus which is hydrogen-bonded to C^4 and A^1 in Figure 1). Existence of the arch for AUCCA is consistent with the observation of enhanced shielding at C^3H5 and H6. Quigley & Rich (1976) mention that ribose 58 is held in the unusual ^2E conformation; likewise, our NMR evidence indicates an unusually high fraction of ^2E conformers at the corresponding position A^1 in AUCCA. If the arch is indeed the class II conformation of AUCCA, we find it reasonable that shielding differences might occur for U^2H1' and C^3H1', both residues corresponding to the unusual stacking arrangement at U^{59} and C^{60} in the tRNA. Shielding effects on H1′ protons are difficult to explain quantitatively, however (Borer et al., 1975), and we offer no explanation at this time for the origin of shielding increases at these positions.

The $J_{1'-2'}$ values reflecting ribose conformation at C^3 indicate that ^3E clearly dominates, and there is no evidence that ^2E forms are present in the class II AUCCA conformations. The position corresponds to C^{60} in the tRNA and is supposed to have the ^2E pucker according to the crystal studies (Stout et al., 1978; Hingerty et al., 1978; Holbrook et al., 1978). The X-ray studies can easily determine ^2E or ^3E conformation because the two require very different distances between adjacent phosphates which are electron rich and easily placed in the electron-density maps. Therefore, the NMR evidence indicates that at least this part of the arch structure does not conform to the class II structures.

There are other plausible models for class II structures, the most attractive being one in which A^1 and A^5 stack upon each other with the other residues looped out in some manner. Precedent for such structures has been established in trinucleoside diphosphates with purines at the ends and pyrimidines, especially uridine, in the middle (Gray et al., 1972; Lee & Tinoco, 1980; M. P. Stone et al., unpublished experiments). Such a model for AUCCA would predict large changes in shielding for A^1 protons upon addition of A^5 to the chain; Table II shows that the A^1 resonances are very insensitive to chain length.

Several experiments are planned to help in building a model for the class II structures. First, we plan to look for resonances in H_2O that might correspond to the C^4-4-amino and A^1-2′-OH protons in slow exchange (see Figure 1a) as predicted by the arch model. Second, we are continuing ^{31}P NMR studies of the AUCCA series. Already we have noticed one of the four phosphorus resonances of AUCCA which is shifted considerably from the others and appears to undergo a transition in its δ vs. T profile (M. P. Stone and P. N. Borer, unpublished results). This could correspond to the hydrogen-bonded phosphate in Figure 1a. We further plan experiments at 500 MHz using newly developed methods in FT NMR to obtain coupling constants and chemical shifts for the 25 other sugar protons ignored in this study. Finally analysis of the series CA, CCA, UCCA, and AUCCA should give

additional information about shielding at the 3′ end of the molecule and allow us to independently confirm all our assignments.

Acknowledgments

We are grateful to Cathy Moore, University of California at Irvine, Dr. Jerry Dallas, University of California at Davis, and Dr. John Wright, University of California at San Diego, for assistance in obtaining some of our NMR spectra.

Appendix

Detailed Assignments. Assignment of H2, H8, H6, H5, and H1′ resonances of AU are given by Davies & Danyluk (1974). Comparison of AU spectra at high temperature with spectra of AUC, AUCC, and AUCCA leads to straightfoward assignment of A^1- and A^5H8 and provides the basis for the remaining assignments. A1- and A^5H2 resonate within 0.03 ppm of each other at 70 °C, but the assignment shown in Figure 4 is most consistent with the AUCC spectra. Also, this A^5 proton is expected to have a greater temperature dependence since its neighbor is C while U is the neighbor of A^1. U^2H6 and -H5 signals are identified by their distinctive 8.1-Hz coupling constants. The H6 and H5 of the two C residues are impossible to distinguish by the incremental assignment scheme. C^4H6 is assigned to the CH6 doublet having the greatest temperature dependence, a consequence of the ring current of A^5. On the other hand, the assignment of C^3H5 and C^4H5 must be regarded as tentative (see Figure 3); we assign the most shielded resonance as C^4H5, again because of the proximity of the A^5 ring. We note that if the assignments were reversed, then the $\Delta\delta$ value for C^3H5 would be ~0.05 ppm larger than that indicated in Table II; this would make an even stronger case for the existence of class II structures for AUCCA.

Referring now to Figure 4 and Table I, we can discuss the H1′ assignments. These are the least securely identified resonances in AUCCA. These are considered individually. *A^1H1′* can be assigned easily in AUCC by comparison with AU and AUC spectra. In AUCCA there is a problem in distinguishing it from A5H1′. We favor the present assignment (Figure 4) as the A^1H1′ δ vs. T profiles are nearly superimposable throughout the whole range of temperature. In further support of our assignment is an examination of the adenosine H1′ coupling constant in the dimer CpA (M. P. Stone and P. N. Borer, unpublished experiments). At 6 °C, the adenosine H1′ proton of CpA shows a coupling constant $J_{1'-2'}$ of <3 Hz. Thus, a coupling of 4.5 Hz (Table I) at this temperature for the analogous A^5 resonance in the pentamer AUCCA is unlikely. If anything, the 3-Hz value should decrease in a longer, more fully stacked, oligomer; we therefore ascribe the 2.6-Hz coupled AUCCA resonance to *A^5H1′*. *U^2H1′* is easily assigned in AUC and AUCC by incremental assignment from AU at high temperature. In each of these three oligomers the U^2 proton has a fairly large value of $J_{1'-2'}$ at low temperature, ≥3 Hz, the largest of the three pyrimidine nucleosides. Upon addition of A^5, this resonance is nearly superimposable with U^2H1′ of AUCC at high temperature. At intermediate temperatures it overlaps severely with the resonance designated as C^4H1′ in Figure 4 and may actually cross over. We decided to interpret these two δ vs. T profiles as meeting but not crossing because this decision allows the larger (2.4-Hz, 6 °C) coupling constant to belong to U^2H1′, consistent with the large J values observed in AU, AUC, and AUCC. We emphasize the possibility that the low-temperature assignment may be incorrect in this case which would ascribe an unusually large $J_{1'-2'}$ value to C^4H1′ (or C^3H1′ as we discuss next). *C^3H1′* is easily identified in AUC but upon addition of C^4 in AUCC becomes much less certain. The AUCC δ vs. T profile designated as C^4H1′ in Figure 4 is very nearly superimposable with C^3H1′ in AUC which would seem to contradict the present assignment. However, the profile denoted as C^3H1′ in AUCC (Figure 4) is very nearly parallel to the putative C^3H1′ profile of AUCCA. One expects addition of A^5 to shift C^3H1′ upfield slightly, consistent with the present assignment. The apparent contradiction just noted is not serious since it is reasonable that the chemical shift of C^3H1′ would become more temperature dependent upon addition of C^4 to AUC. *C^4H1′* has very little temperature dependence of chemical shift in AUCC in the present assignment and might be expected to have the same sort of δ vs. T profile as C^3H1′ in AUC; these are both 3′-terminal C residues with a pyrimidine nucleotide as the 5′ neighbor. Addition of A^5 should have a dramatic effect on this profile because of the large ring-current shielding of adenine. The present assignment gives a greater temperature dependence of chemical shift to C^4H1′ and allows it to be slightly more shielded than C^3H1′ at high temperature. As was noted above in the discussion of U^2H1′, the integrity of the C^4H1′ assignment is ambiguous at low temperature due to the overlap and possible crossover with U^2H1′.

These assignments are of course less secure than are obtained by direct methods such as selective deuteration. We recognize that there is particular confusion surrounding the identification of U^2, C^3, and C^4H1′. While the present assignments are probably correct, a plausible alternative in Figure 4 interchanges C^3 and C^4 at high temperature and possibly interchanges C^3 and U^2 at low temperature. These possibilities increase the aberrant $\Delta\delta$ values in Table II and would add further support to the existence of class II conformations similar to the arch model. The interchange of C^3 and U^2H1′ at low temperature would increase the fraction of the ^{2}E conformation at C^3 as predicted by the arch structure. While these possibilities are attractive in light of the arch model, we prefer to maintain the conservative and self-consistent assignments given in Figure 4.

Supplementary Material Available

Two tables describing the temperature dependence of H1′–H2′ coupling constants and chemical shifts for AU and AUC (2 pages). Ordering information is given on any current masthead page.

References

Borer, P. N. (1975) *Handbook of Biochemistry and Molecular Biology, Nucleic Acids* (Fasman, G. D., Ed.) Vol. 1, p 389, CRC Press, Cleveland, OH.

Borer, P. N., Kan, L. S., & Ts'o, P. O. P. (1975) *Biochemistry 14*, 4847.

Davies, D. B., & Danyluk, S. S. (1974) *Biochemistry 13*, 4417.

Dhingra, M. M., & Sarma, R. H. (1979) in *Stereodynamics of Molecular Systems* (Sarma, R. H., Ed.) p 15, Pergamon Press, New York.

Gray, D. M., Tinoco, I., Jr., & Chamberlin, M. J. (1972) *Biopolymers 11*, 1235.

Hingerty, B., Brown, R. S., & Jack, A. (1978) *J. Mol. Biol. 124*, 523.

Holbrook, S. R., Sussman, J. L., Warrant, R. W., & Kim, S. H. (1978) *J. Mol. Biol. 123*, 631.

Kan, L. S., Ts'o, P. O. P., Sprinzl, M., van der Haar, F., & Cramer, F. (1977) *Biochemistry 16*, 3143.

Kearns, D. R. (1977) *Annu. Rev. Biophys. Bioeng. 6*, 477.

Klee, C. B., & Singer, M. F. (1967) *Biochem. Biophys. Res. Commun. 29*, 356.
Lee, C. H., & Tinoco, I., Jr. (1980) *Biophys. Chem. 11*, 283.
McFarland, G. D., & Borer, P. N. (1979) *Nucleic Acids Res. 7*, 1067.
Prestegard, J. H., & Chan, S. I. (1969) *J. Am. Chem. Soc. 91*, 2843.
Quigley, G. C., & Rich, A. (1976) *Science (Washington, D.C.) 194*, 796.
Reid, B. R., & Hurd, R. E. (1977) *Acc. Chem. Res. 10*, 396.
Rich, A., Quigley, G. C., & Wang, A. H. J. (1979) in *Stereodynamics of Molecular Systems* (Sarma, R. H., Ed.) p 315, Pergamon Press, New York.
Stout, C. D., Mizuno, H., Rao, S. T., Swaminathan, P., Rubin, J., Brennan, T., & Sundaralingam, M. (1978) *Acta Crystallogr. B34*, 1529.
Sundaralingam, M. (1974) *Struct. Conform. Nucleic Acids Protein-Nucleic Acid Interact., Proc. Annu. Harry Steenbock Symp., 4th*, 487.
Ts'o, P. O. P. (1974) in *Basic Principles in Nucleic Acid Chemistry* (Ts'o, P. O. P., Ed.) Vol. I, p 453, Academic Press, New York.
Uhlenbeck, O. C., Borer, P. N., Dengler, B., & Tinoco, I., Jr. (1973) *J. Mol. Biol. 73*, 483.
Van Geet, A. L. (1968) *Anal. Chem. 40*, 2227.
Van Geet, A. L. (1970) *Anal. Chem. 42*, 679.

Poly(adenosine diphosphoribose) Synthesis in Ultraviolet-Irradiated Xeroderma Pigmentosum Cells Reconstituted with *Micrococcus luteus* UV Endonuclease†

Nathan A. Berger* and Georgina W. Sikorski

ABSTRACT: Synthesis of DNA and poly(adenosine diphosphoribose) [poly(ADPR)] was examined in permeabilized xeroderma pigmentosum lymphoblasts (XP3BE) before and after UV irradiation and in the presence and absence of *Micrococcus luteus* UV endonuclease. *M. luteus* UV endonuclease had no effect on the level of DNA or poly(ADPR) synthesis in control, unirradiated cells. UV irradiation caused a decrease in replicative DNA synthesis without any significant change in poly(ADPR) synthesis. In UV-irradiated cells treated with *M. luteus* UV endonuclease, DNA synthesis was restored to a level slightly greater than in the unirradiated control cells, and poly(ADPR) synthesis increased by 2- to 4-fold. Time–course studies showed that the UV endonuclease dependent poly(ADPR) synthesis preceded the endonuclease-dependent DNA synthesis. Inhibition of endonuclease-dependent poly(ADPR) synthesis with 3-aminobenzamide, 5-methylnicotinamide, or theophylline produced a partial inhibition of the endonuclease-dependent DNA synthesis. Conversely, inhibition of the endonuclease-dependent DNA synthesis with dideoxythymidine triphosphate, phosphonoacetic acid, or aphidicolin had no effect on the endonuclease-dependent poly(ADPR) synthesis. These studies show that stimulation of poly(ADPR) synthesis in UV-irradiated cells occurs subsequent to the DNA strand breaks created by the specific action of the UV endonuclease on UV-irradiated DNA. The effect of the inhibitors of poly(ADPR) synthesis in UV-irradiated cells indicates that the endonuclease-stimulated DNA synthesis is dependent in part on the prior synthesis of poly(ADPR).

Poly(adenosine diphosphoribose) is synthesized from NAD^+ by poly(ADPR)[1] polymerase, which is a tightly bound chromosomal enzyme activated when cells are treated with various agents that damage DNA (Miller, 1975; Hayaishi & Ueda, 1977; Davies et al., 1977; Berger et al., 1979a–c). The rapid synthesis and degradation of ADP-ribose polymers in the nucleus have the potential for causing drastic but reversible alterations in chromatin conformation. Since poly(ADPR) synthesis increases in response to DNA damage, it was proposed that poly(ADPR) might be involved in the DNA repair process, altering chromatin structure so as to make regions of DNA damage more readily accessible to the enzymes of DNA repair (Miller, 1975; Davies et al., 1977; Cleaver, 1978; Berger et al., 1979c). This proposal has been partially confirmed by the demonstration that inhibitors of poly(ADPR) synthesis interfere with the ability of cells to recover and proliferate following DNA damage (Durkacz et al., 1980). In addition, cells made NAD^+ deficient by nicotinamide starvation are unable to carry out unscheduled DNA synthesis after treatment with *N*-methyl-*N'*-nitro-*N*-nitrosoguanidine (MNNG); they are also unable to reseal DNA strand breaks after treatment with dimethyl sulfate (Durkacz et al., 1980; Jacobson et al., 1980).

We have shown that cells from normal human donors develop an increase in poly(ADPR) synthesis after treatment with various DNA damaging agents including MNNG, (*N*-acetoxyacetylamino)fluorene, bleomycin, and UV irradiation

† From the Department of Medicine, Washington University School of Medicine, Division of Hematology/Oncology, The Jewish Hospital of St. Louis, St. Louis, Missouri 63110. *Received July 30, 1980.* This work was supported by National Institutes of Health Grants GM26463 and CA23986 and American Cancer Society Grant CH-134. Cell culture medium was prepared in a Cancer Center Facility funded by the National Cancer Institute. N.A.B. is a Leukemia Society of America Scholar.

[1] Abbreviations used: ADPR, adenosine diphosphoribose; AP, apyrimidinic; aCTP, cytosine arabinoside triphosphate; d_2TTP, dideoxythymidine triphosphate; Hepes, 4-(2-hydroxyethyl)-1-piperazineethanesulfonic acid; MNNG, *N*-methyl-*N'*-nitro-*N*-nitrosoguanidine; NAD, nicotinamide adenine dinucleotide; UV, ultraviolet; XP, xeroderma pigmentosum; Tris, tris(hydroxymethyl)aminomethane; EDTA, ethylenediaminetetraacetic acid.

0006-2960/81/0420-3610$01.25/0